Available online at www.sciencedirect.com
SCIENCE DIRECT®
Journal of Solid State Chemistry 178 (2005) 2897–2906
JOURNAL OF SOLID STATE CHEMISTRY
www.elsevier.com/locate/jssc

Structural models for intergrowth structures in the phase system Al_2O_3–TiO_2

Stefan Hoffmann[a,*], Stefan T. Norberg[b], Masahiro Yoshimura[a]

[a]*Materials and Structures Laboratory, Tokyo Institute of Technology, 4259 Nagatsuta-cho Midori-ku, Yokohama 226-8503, Japan*
[b]*Ceramics Research Laboratory, Nagoya Institute of Technology, 10-6-29 Asahigaoka, Tajimi, Gifu 507-0071, Japan*

Received 28 April 2005; received in revised form 23 June 2005; accepted 1 July 2005

Abstract

The phase system Al_2O_3–TiO_2 was investigated in the compositional range from 48:52 to 62:38 mol% Al_2O_3:TiO_2. The samples were prepared by melting the binary oxides in an arc-imaging furnace and the obtained samples were examined by powder X-ray diffraction. The recorded powder patterns could be interpreted in terms of intergrowth structures consisting of two basic building blocks, which were deduced from the known crystal structures of β-Al_2TiO_5 and $Al_6Ti_2O_{13}$. The structure of a new ordered compound with the formula $Al_{16}Ti_5O_{34}$ is proposed. The thermal stability was estimated from DTA and tempering experiments and showed that all prepared samples decompose at temperatures around 800 °C into the binary oxides corundum and titania.
© 2005 Elsevier Inc. All rights reserved.

Keywords: Aluminum titanate; Al_2O_3–TiO_2 phase system; Intergrowth structure; DTA

1. Introduction

Pseudo-binary phase diagrams consisting of titania and an oxide of a trivalent metal with a similar ionic radius were investigated extensively after the fundamental structural principle for titanium suboxides were discovered [1]. Nevertheless, relatively little attention has been paid to the system Al_2O_3–TiO_2 for which some unknown high temperature phases were reported 1968 by Goldberg [2] in the compositional range from 60 to 66 mol% Al_2O_3, all according to the X-ray powder patterns and microscopic results on etched specimens. These compounds were only stable in a narrow high-temperature range below which they decompose. Goldberg's experimental results are summarized in Fig. 1.

With respect to the structural chemistry only the structure of β-Al_2TiO_5 [3] was known for a long time, which adopts the pseudobrookite [4] structure type. This compound has been studied extensively because of its physical properties. It has a low thermal expansion [5], which makes it interesting for applications where sudden temperature changes are encountered. At room temperature the compound is metastable with a noticeable decomposition into alumina and titania at elevated temperatures (above 750 °C, [6–10]) and at even higher temperatures it becomes thermodynamically stable (above 1300 °C). Furthermore, the cation distribution was subject of investigations by single crystal X-ray crystallography [11] and transmission electron microscope (TEM) [12]. A still open question is whether a high-temperature phase of Al_2TiO_5 structurally different from the known low temperature phase exists, i.e. does the suggested α-Al_2TiO_5 phase [13] exist, something which so far has not been proved [14]. An excellent review dealing with β-Al_2TiO_5 and the phase system Al_2O_3–TiO_2 was published 1989 by Thomas and Stevens [15].

Recent TEM investigations [16] and the structure determination of a new compound with the formula

*Corresponding author. Fax: +81 45 924 5358.
E-mail address: stefan598@aol.com (S. Hoffmann).

0022-4596/$ - see front matter © 2005 Elsevier Inc. All rights reserved.
doi:10.1016/j.jssc.2005.07.001

$Al_6Ti_2O_{13}$ [17] encourage us to re-investigate the phase system in the range from 48:52 to 62:38 mol% Al_2O_3:TiO_2 by means of powder X-ray diffraction which unlike the above-mentioned methods gives information about the whole sample. Particular attention was paid to sample preparation and the evaluation of the powder patterns, which suffers from strong overlap of reflections due to the formation of similar structures. Furthermore the thermal stability of the compounds formed in that compositional range was investigated by DTA and isothermal annealing.

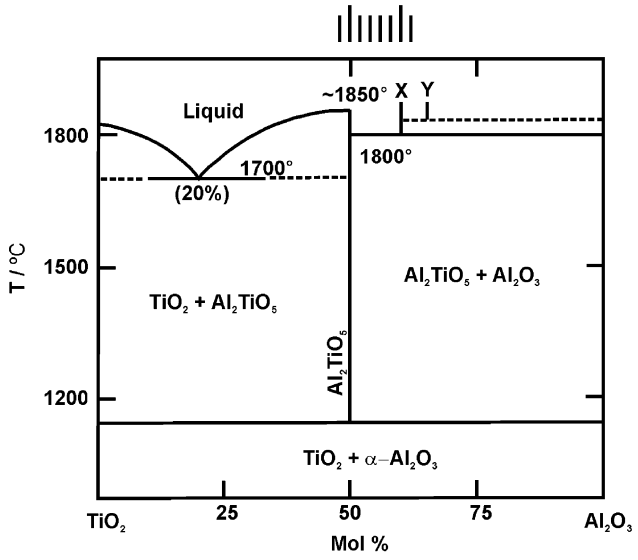

Fig. 1. Redrawn phase diagram proposed by Goldberg in 1968 [2] and examined compositions marked by bars above from 48 to 62 mol% Al_2O_3.

2. Experimental

2.1. Synthesis

Eight mixtures consisting of the oxides Al_2O_3 and TiO_2 in a molar ratio given in Table 1 were prepared. α-Al_2O_3 (Sumitomo Chemicals type AKP-30 high purity) and TiO_2 (High Purity Chemicals Kōjundo Kagaku Kenkyū 99.99%, consisting of 96 wt% rutile and 4 wt% anatase according to X-ray powder pattern) were weighted and afterwards thoroughly mixed in a corundum mortar using ethanol, then dried in air and melted in an arc-imaging furnace which basically consists of a water cooled copper plate and an optical system which collects and focuses the light from a xenon lamp on the sample (see [18] for a sketch of the apparatus). First the mixed oxides were completely melted by open a shutter situated between the lamp and the sample. Then the obtained spherical specimens with a diameter of 2–3 mm were turned over and again melted to ensure a complete melting. Samples prepared in that way will referred here after as "as-quenched". To obtain better crystallized samples the globules were once more melted followed by a 15 min soaking period right below the solidification point which was indicated by deformation of the sample surface as well as a change in reflectivity. Aware of the quite subjectivity of this method simply due to the lack of a temperature measurement always three specimens of the same composition were prepared and analyzed in order to get as homogeneously crystallized samples as possible. However, no significant differences were seen for different samples with same molar composition.

Table 1
Summary of conducted experiments with sample compositions, thermal treatment, and result of powder pattern fitting (A = annealing in the arc-imaging furnace for 15 min, IG = intergrowth structure due to residual intensity after powder pattern fitting)

Composition Al_2O_3:TiO_2 (mol%)	Thermal treatment	Product identified by powder X-ray diffraction
48:52	A	β-Al_2TiO_5, rutile, traces of Al_2O_3
50:50	A	β-Al_2TiO_5, $Al_6Ti_2O_{13}$, traces of Al_2O_3, IG
52:48	A	β-Al_2TiO_5, $Al_6Ti_2O_{13}$, traces of Al_2O_3, IG
54:46	A	β-Al_2TiO_5, $Al_6Ti_2O_{13}$, traces of Al_2O_3, IG
56:44	A	β-Al_2TiO_5, $Al_6Ti_2O_{13}$, traces of Al_2O_3, IG
58:42	A	β-Al_2TiO_5, $Al_6Ti_2O_{13}$, traces of Al_2O_3, IG
60:40	A	$Al_6Ti_2O_{13}$, traces of Al_2O_3, β-Al_2TiO_5, IG
60:40	Starting from powder Al_2O_3 and TiO_2, 1000 °C for 24 h	α-Al_2O_3 and rutile (no reaction)
60:40	Starting from powder Al_2O_3 and TiO_2, 1400 °C	β-Al_2TiO_5, α-Al_2O_3, traces of rutile
60:40	As-quenched from melt	$Al_6Ti_2O_{13}$, traces of α-Al_2O_3, β-Al_2TiO_5, IG
	And annealing at 800 °C for 12 h	No change
	Further annealing at 800 °C for 24 h	No change
	Further annealing at 900 °C for 54 h	$Al_6Ti_2O_{13}$, α-Al_2O_3, rutile, IG
60:40	As-quenched from melt and annealed at 1000 °C for 24 h	$Al_6Ti_2O_{13}$, α-Al_2O_3, rutile, IG
60:40	As-quenched from melt and annealed at 1400 °C for 24 h	β-Al_2TiO_5, α-Al_2O_3, traces of rutile
62:38	A	$Al_{16}Ti_5O_{36}$, traces of IG

2.2. Annealing experiments

To evaluate the thermal stability and to improve the crystallinity of the new compound $Al_6Ti_2O_{13}$ several annealing experiments were conducted starting from a mixture of alumina and titania powder in the molar ratio 3:2 as well as samples which were already melted in the arc-imaging furnace. All powders were mixed and pressed into pellets (diameter 20 mm, thickness about 2 mm, mass about 1.5 g, and pressure 30 kg/cm^2). Both types of samples with the same chemical composition were placed in alumina boats and heated to 1000 °C (KDF S-70, canthal furnace) or 1400 °C (Nishimura Kogyo, super canthal furnace) for 24 h. In addition five as-quenched globules were inserted in a pre-heated furnace, annealed for 15 h at 1400 °C and then quenched in a water bath. Finally, prolonged annealing with intermediate grinding using as-quenched specimens was tried out. The specimens were first heated to 800 °C for 12 h, then cooled down, grinded for 30 min in ethanol, examined by X-ray powder diffraction, then pressed again into a pellet, heated for 24 h to 800 °C, again examined by powder X-ray powder diffraction, and at the end heated for 54 h to 900 °C.

2.3. DTA

Several DTA experiments (Materials Analysis and Characterization TG-DTA 2000) were carried out using different heating rates, sample amounts, and grain sizes. Samples prepared from the mixtures Al_2O_3:TiO_2 with a molar ratio 50:50, 60:40, and 62:38 were placed in a platinum crucible and heated up to 1400 °C two times. The resulting powder was examined by X-ray powder diffraction. Both as-quenched and annealed samples were examined.

2.4. Powder X-ray diffraction and evaluation

After melting the globules were crushed in a corundum mortar and then grinded for 30 min in ethanol. The powders had a gray to bluish-grey appearance. A glass sample holder with a quadratic dip (0.2 mm depth) was front-loaded and measured with an X-ray powder diffractometer (Rigaku RINT 2000, Cu$K\alpha$ radiation, 200 mA 50 KV) typically in the 2θ-range of 3–53°, with a scan speed of 0.55°/min, and a step width of 0.02° (1 1/2 h measuring time). Smaller samples amounts of around 10 mg as they were obtained from DTA were simply dispersed in ethanol and placed on a glass plate.

The recorded patterns were compared with reported patterns from ICCD. After the identification of the crystalline compounds the patterns were fitted with structural models for α-Al_2O_3, TiO_2 (rutile), and β-Al_2TiO_5 taken from references [11,19,20] as well as the recently discovered $Al_6Ti_2O_{13}$ [17] using the program *FULLPROF*2000 [21]. The parameters for the zero-point shift, background, line shape, and unit cell were refined whereas the atomic coordinates and the isotropic atomic displacement parameters were fixed.

For the calculation of the powder patterns for derived structural models the known structure of $Al_6Ti_2O_{13}$ was transferred into a model in space group P1 by means of the program DIAMOND [22]. The resulting atom positions were used as input for the program DIFFaX, which allows a convenient calculation of powder diagrams for layered structures [23]. The space groups of ordered models were determined by the subprogram ADDSYM contained in the program package PLATON [24].

3. Results and discussion

3.1. Powder fitting for $Al_6Ti_2O_{13}$

For the determination of physical properties the synthesis of well crystalline and pure samples is essential which can be quickly estimated by fitting the recorded X-ray powder patterns. A typical powder XRD pattern of a melted and annealed sample obtained from a mixture Al_2O_3:TiO_2 3:2 mol is shown in Fig. 2. The identified crystalline products are $Al_6Ti_2O_{13}$ as the main component, β-Al_2TiO_5, and α-Al_2O_3.

The visual inspection of the fitted powder X-ray pattern (Fig. 2) revealed that the assumption of three crystalline products is not sufficient to describe all features of the recorded pattern. Most obviously the four strongest reflections of $Al_6Ti_2O_{13}$ 020, 110, 024, and 200 are not well fitted. The 024 reflection which is the only one out of these four strong reflections with $l \neq 0$ shows two shoulders (inset Fig. 2). From this observation and results from TEM investigations [16] we conclude that in addition intergrowth structures (IG) were formed characterized by almost the same length of a and b axis but different c-axis.

The lattice parameter refinement for the compound $Al_6Ti_2O_{13}$ for three different samples using the 2θ-range from 12° to 90° gave the average values of $a = 3.633(4)$ Å, $b = 9.322(4)$ Å, and $c = 12.490(4)$ Å. These values are approximately 0.5% smaller than those earlier determined for a single crystal [17].

The calculated powder pattern for $Al_6Ti_2O_{13}$ was compared with the powder pattern of the reported high-temperature phase of Al_2TiO_5 (α-Al_2TiO_5 [13]) but there was no significant overlap. This is in agreement with the results of Azimov et al. [14,25] who could not obtain the high-temperature phase using a solar furnace.

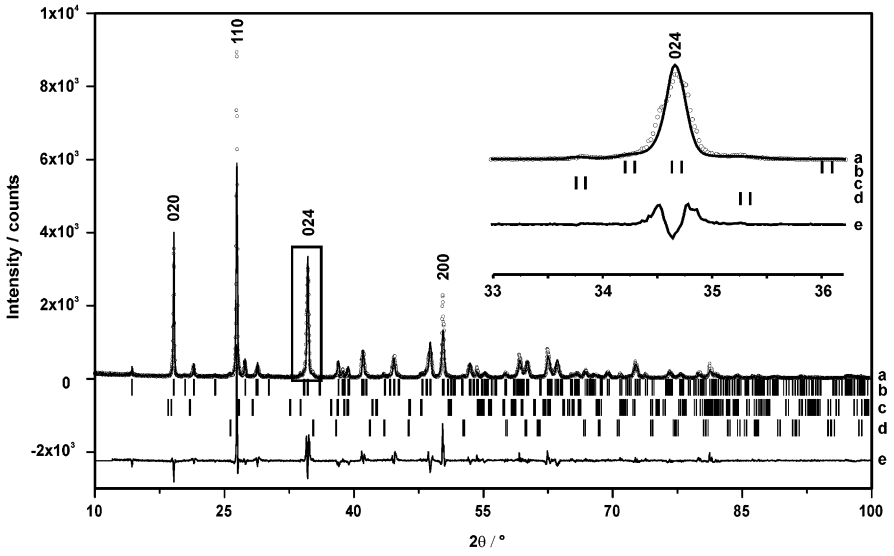

Fig. 2. X-ray powder pattern fit for an annealed sample with the nominal composition Al_2O_3:TiO_2 60:40 mol% and an enlarged part shown in the inlet: (a) recorded pattern as hollow circles and calculated pattern as solid line; (b) positions of Bragg reflections for $Al_6Ti_2O_{13}$; (c) positions of Bragg reflections for β-Al_2TiO_5; (d) positions of Bragg reflections for corundum; (e) difference between measured and calculated intensity.

3.2. Thermal stability

The thermal behavior was investigated by DTA and conventional annealing at temperatures of 800, 900, 1000, and 1400 °C.

For $Al_6Ti_2O_{13}$ two kinds of samples one as-quenched and one annealed were examined by DTA. Both samples consist mainly of $Al_6Ti_2O_{13}$, traces of α-Al_2O_3 and unidentified compounds with reflections strongly overlapping that of $Al_6Ti_2O_{13}$. The observed thermal effects are quite small (10–50 mg sample weight) and comparable for both samples. The recorded DTA traces for the annealed sample are given in the Supplementary Material.

During the first heating a broad exothermic effect starting at 1100 °C can be seen followed by an endothermic between 1300 and 1400 °C. During the second heating this behavior is less pronounced but the endothermic effect is still clearly observable. All examined samples change their color from grey to almost white.

The powder X-ray diffraction revealed that after thermal treatment at 1400 °C the compound $Al_6Ti_2O_{13}$ decomposes and the product composition depends on the heating rate and the way the sample was prepared for the DTA experiment. Simply crushed and slightly grinded material consist of $Al_6Ti_2O_{13}$, β-Al_2TiO_5, and α-Al_2O_3 after the treatment with a heating rate of 10 or 20 K/min, and traces of rutile whereas a slower heating with 5 K/min yielded a powder with a higher α-Al_2O_3 and rutile content but a smaller $Al_6Ti_2O_{13}$ content. Well grinded material (10 or 30 min in ethanol) is converted to β-Al_2TiO_5, α-Al_2O_3, and traces of rutile at heating rates of 5, 10, and 20 K/min.

For samples obtained from a mixture Al_2O_3:TiO_2 with a molar ratio 62:38 shows a quite similar thermal behavior during heating. The product after heating consists of β-Al_2TiO_5, α-Al_2O_3, and rutile according to the X-ray powder pattern. Further information are given in the Supplementary Material.

For comparison a sample of melt synthesized β-Al_2TiO_5 was also subjected to DTA. The first thermal effect is a broad exothermic peak between 800 and 1000 °C followed by a weak endothermic effect at around 1300 °C. The product after cooling is β-Al_2TiO_5 identified by X-ray diffraction. Further information are given in the Supplementary Material.

Annealing of an as-quenched specimen at 800 °C with intermediate grinding for a total dwelling time of 36 h does not lead to a noticeable decomposition whereas at 900 and 1000 °C newly formed α-Al_2O_3 and rutile can be observed beside $Al_6Ti_2O_{13}$. The quality of the fit for the pattern resulted from $Al_6Ti_2O_{13}$ did not improve significantly after annealing. At 1400 °C only β-Al_2TiO_5 and α-Al_2O_3 can be detected and no difference between fast heating (inserting the sample in the pre-heated furnace) and slow heating can be recognized.

If α-Al_2O_3 and rutile in a molar ratio of 60:40 are heated together to 1000 °C for 24 h no reaction can be observed. At 1400 °C β-Al_2TiO_5 and α-Al_2O_3 can be detected as crystalline products.

For β-Al_2TiO_5 the observed disorder in the cation lattice was connected to the thermal instability of the compound at temperatures below about 1300 °C [11].

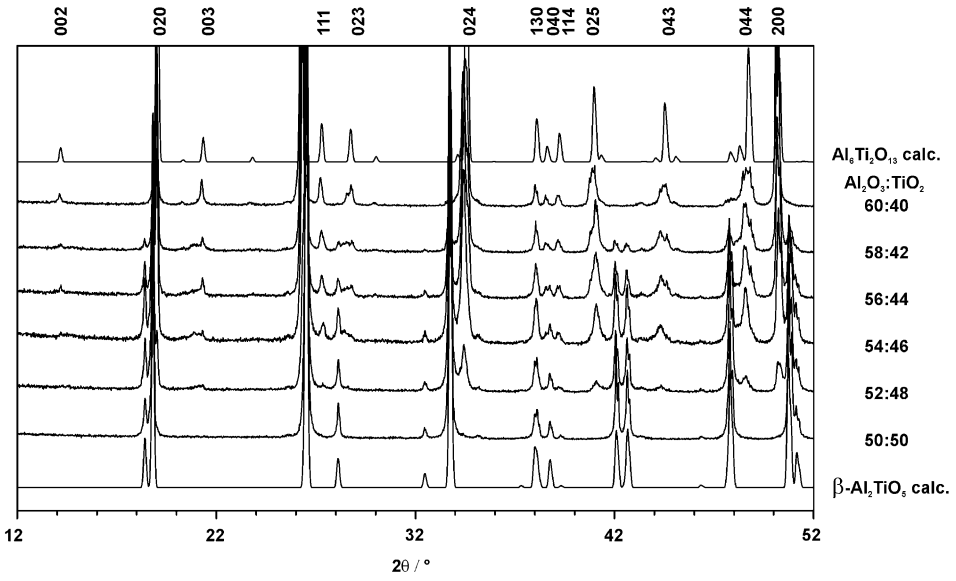

Fig. 3. Recorded X-ray powder patterns for the compositional range 50:50 to 60:40 mol% Al_2O_3:TiO_2 and for comparison the calculated patterns for β-Al_2TiO_5 (below) and $Al_6Ti_2O_{13}$ (above) with Miller's indices for $Al_6Ti_2O_{13}$ given above the diagram.

Later calorimetric measurements revealed that this type of compound is "entropy-stabilized" [26]. The same seems to be true for the new compound $Al_6Ti_2O_{13}$, which decomposes into α-Al_2O_3 and rutile at temperatures higher than 800 °C. In fact there is no DTA signal directly connected with the decomposition in this temperature range which suggests that the conversion is sluggish, even though the following thermal events at higher temperatures remind of the crystallization of β-Al_2TiO_5 from amorphous precipitates [27] where first the crystallization of alumina and titania takes place at around 1000 °C connected with an exothermal signal and these two compounds react at around 1320 °C to form β-Al_2TiO_5 (endothermic). At temperature higher than accessible with our DTA apparatus it is supposed that the mixture of β-Al_2TiO_5 and corundum further reacts to $Al_6Ti_2O_{13}$.

The eutectoid decomposition was also observed for the structurally unknown compounds suggested by Goldberg [2] and therefore it is concluded that $Al_6Ti_2O_{13}$ is one of the proposed compounds (Fig. 1).

3.3. Compositional variation

To get more information about the phase system near the composition of $Al_6Ti_2O_{13}$ six samples with less alumina and one sample with higher alumina content were prepared in the same way by annealing in the arc-imaging furnace. All results are summarized in Table 1.

When a mixture of corundum and titania with a molar ratio of 48:52 is melted samples consisting of β-Al_2TiO_5 and traces of rutile were obtained. An increase of the alumina content to 50 mol% leads to additional weak reflections, which can be assigned to $Al_6Ti_2O_{13}$. A further small increase of 2 mol% clearly facilitated the formation of the new compound $Al_6Ti_2O_{13}$ as indicated by the 003 reflection at $2\theta = 21.3°$ (Fig. 3). A stepwise increase until 60 mol% alumina causes an increase of the intensity owing to the compound $Al_6Ti_2O_{13}$ whereas the intensity of the reflections of β-Al_2TiO_5 become weaker and finally almost disappears completely at 60 mol% alumina. A closer inspection of the weaker reflections assigned to $Al_6Ti_2O_{13}$ shows that reflections indexed by Miller's indices hkl and $l \neq 0$ are considerably broadened and even shifted with respect to the powder pattern calculated from the structural model determined by X-ray single crystal analysis (Fig. 3). In addition all mentioned problems described for the powder pattern fitting for $Al_6Ti_2O_{13}$ were encountered.

Samples with a nominal molar composition Al_2O_3:TiO_2 62:38 show a quite distinguished pattern for the weak reflections as shown in Fig. 4. The 002 reflection of $Al_6Ti_2O_{13}$ seems to be shifted to lower 2θ angles and the 003 and 023 to higher values.

3.4. Structure modeling

The results from X-ray powder diffraction suggest the formation of new compounds as already described by other authors [2,16]. Due to the recently solved structure of $Al_6Ti_2O_{13}$ and results from HRTEM experiments which suggest the formation of IG in the range 50:50–70:30 it was tried to assembled new crystal structures and compare the calculated X-ray powder patterns for those models with the experimental ones.

First the known crystal structures of $Al_6Ti_2O_{13}$ and β-Al_2TiO_5 were compared (Fig. 5). Both compounds

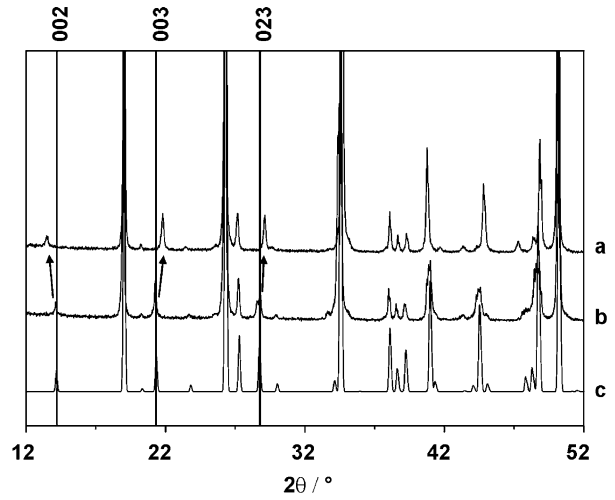

Fig. 4. Recorded X-ray powder patterns for the compositions Al_2O_3:TiO_2: (a) 62:38 mol% and (b) 60:40 mol% and comparison with a calculated pattern for (c) $Al_6Ti_2O_{13}$. The most obvious shifts are marked with arrows and the above given Miller's indices refer to the reflections of $Al_6Ti_2O_{13}$.

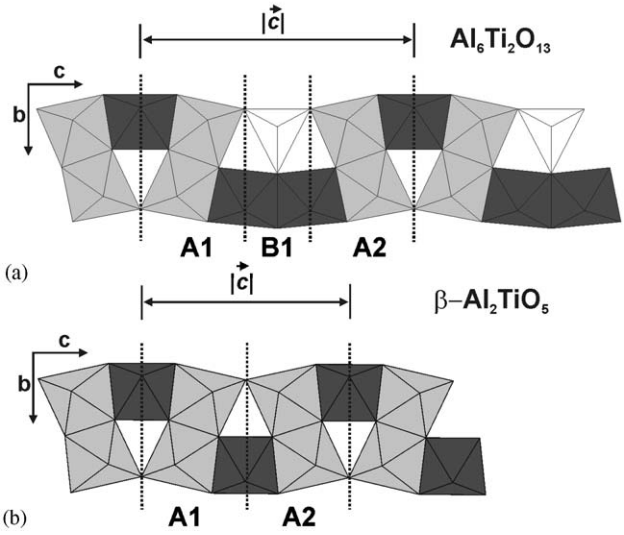

Fig. 5. Comparison of polyhedra chains found in the two known crystal structures of (a) $Al_6Ti_2O_{13}$ and (b) β-Al_2TiO_5: The dotted lines mark the basic building blocks, which are labeled with capitals.

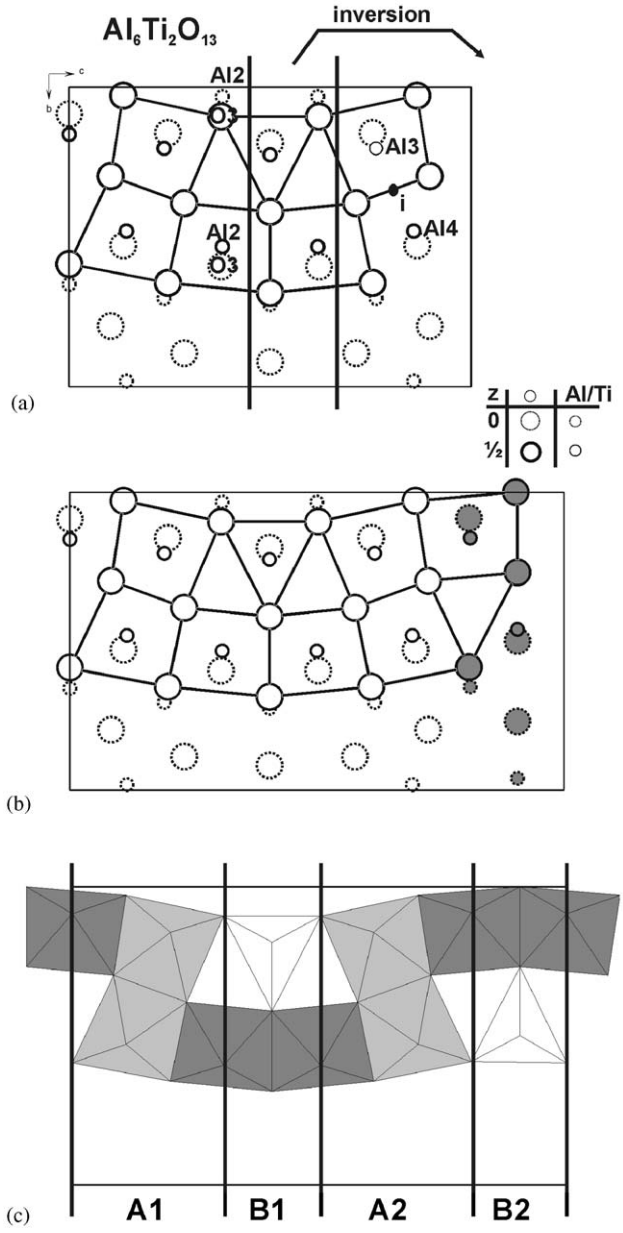

Fig. 6. Generation of the four basic building blocks: (a) The unit cell of $Al_6Ti_2O_{13}$ projected along a with all atoms needed to build up the structure in SG P1. The part of the structure between the two solid lines has to be inverted at the marked inversion centre to get a complete set of building blocks. The small table to the right gives the fractional z parameter for all atoms. (b) All 52 atoms are shown which define the four basic building blocks. The gray atoms were generated by inversion. (c) Polyhedra representation of the generated chain divided into four basic building blocks, which are labelled below.

crystallize in the orthorhombic crystal system with almost the same length of the a- and b-axis whereas the c-axis of $Al_6Ti_2O_{13}$ is longer. The observed c-axis length of 12.554(6) Å is in fact close to the previously reported of 12.4 Å as suggested from HRTEM studies [16]. The characteristic structural element of both structures is an infinite double chain running along c as it can be seen in Fig. 5 where segments with the length of $2c$ are shown.

The translational period of a chain in β-Al_2TiO_5 can be divided into two basic units as indicated in Fig. 5b which repeat in an *A1A2A1A2* .... fashion along c. In $Al_6Ti_2O_{13}$ these two basic units can also be identified. In addition a new unit is found always situated between an A1 and A2 unit. This can be described as an *A1B1A2A1B1A2*... sequence (Fig. 5a).

On the basis of the described similarities building blocks were generated starting from the crystal structure of $Al_6Ti_2O_{13}$. Fig. 6a shows all atoms needed to describe the structure of $Al_6Ti_2O_{13}$ in space group P1. To

increase the flexibility of the model a second B-type block was generated by inversion of the B1 block as indicated in Fig. 6a. The inversion centre was defined by the center of a straight line connecting the atoms Al3 and Al4 (atoms label according to [17]). The result of this operation is shown in Fig. 6b where all 52 atoms defining the whole model are drawn. The polyhedra representation is shown in Fig. 6c as well as four basic unit blocks which already define a possible structural model with the sequence *A1B1A2B2* … . The length of the A1 and A2 block is slightly different because in the original structure of $Al_6Ti_2O_{13}$ the A2 blocks is always followed by an A1 block. To simplify the model for both blocks a unique length of 4.769 Å was assumed. The B-type block has a length of 3.017 Å. Furthermore the allowed transitions are fixed to be A1 and B1 can only be followed by B1 or A2 and A2 and B2 only by A1 or B2. The crystallographic data are given in the Supplementary Material.

With these two types of building blocks structures in the compositional range from M_3O_5 (only A blocks, M = Al, Ti) to M_2O_3 (only B blocks) can be assembled. M_3O_5 represents the structure of pseudobrookite whereas the stacking of only B blocks leads to a structure, which is built up of five- and sixfold coordinated cations. The determined space group is Amm2 and the Pearson symbol is oA10. So far this new structure could not be assigned to a parent structure.

To assure the validity the structure of β-Al_2TiO_5 and $Al_6Ti_2O_{13}$ were built up and the corresponding powder patterns were calculated with the program DIFFaX. The comparison with experimental powder patterns proved the correctness of the generated building blocks.

3.5. Disordered models derived from $Al_6Ti_2O_{13}$

As described before some of the recorded reflections of $Al_6Ti_2O_{13}$ show a deviation from the pattern, which was calculated using the structural model derived from single crystal X-ray structure determination. The structural similarity between $Al_6Ti_2O_{13}$ and β-Al_2TiO_5 which both consist of similar building blocks (A-type) implies the possible formation of stacking faults. Starting from $Al_6Ti_2O_{13}$ with the stacking sequence *A1B1A2A1B1A2*… (see Fig. 5a) the transition from A1 to A2 was set to occur with 10%, 20%, and 30% probability and in a second series the transition from B1 to B1 was introduced as deviation from the ordered model of $Al_6Ti_2O_{13}$. The calculated patterns for ordered $Al_6Ti_2O_{13}$ and the models are shown in Fig. 7.

The introduced faults lead to a systematic shift and broadening of all reflections with Miller's indices *hkl* and $l \neq 0$ whereas all reflections with *hk*0 do not change their positions. For instance, an increase of the A-block content cause a shift to lower 2θ values and a broadening of the 003, 023, and 043 reflections as observed in the experiment (see Fig. 3). The 024 and 044 reflections are also gradually shifted to lower 2θ values. For the reflections 025 and 111 a shift to higher 2θ values is observed. These trends are reverted when an additional B1–B1 transition is applied to the model (Fig. 8).

Similar simulations were done starting from the structure of β-Al_2TiO_5 and introducing a transition from an A block to a B block. It was found that already at a 20% transition probability the 002 reflection disappears. In contrast the experimental powder pattern

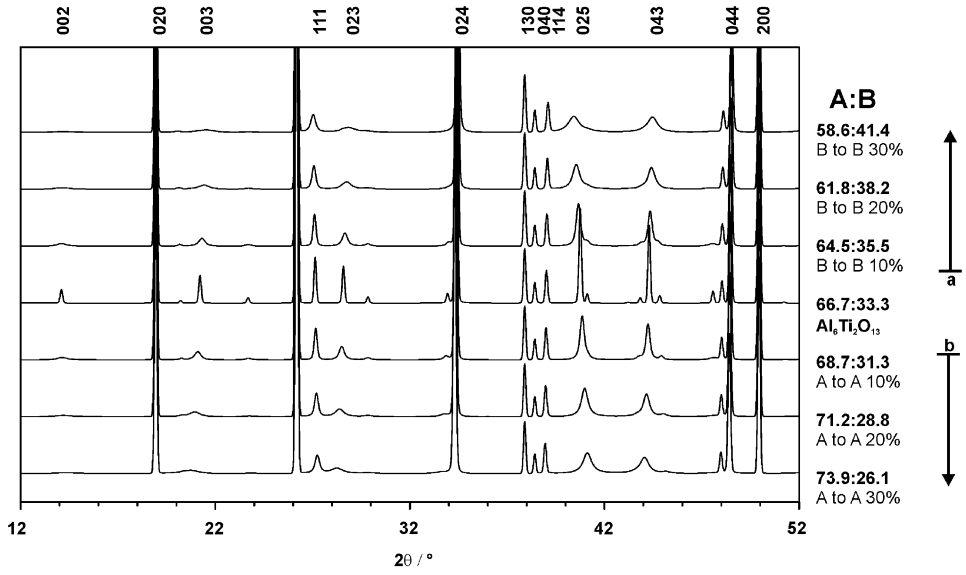

Fig. 7. Calculated X-ray powder patterns for ordered $Al_6Ti_2O_{13}$ (middle) with Miller's indices given above and two types of disorder: (a) An additional transition (transition probability is given) from B1 to B1 is introduced which increase the content of alumina as indicated by the percentage of B blocks. (b) The change of the powder pattern with an increasing content of A blocks is shown. This corresponds to the formation of segments similar to the chain found in β-Al_2TiO_5 which can be described by an *A1A2A1A2*… stacking.

of a sample with a molar ration of Al_2O_3:TiO_2 58:48 still shows this reflection (Fig. 3). Therefore, it is concluded that β-Al_2TiO_5 exhibits no significant intergrowth with B type blocks whereas the structure of $Al_6Ti_2O_{13}$ seems to be able to form stacking faults.

3.6. A new compound: $Al_{16}Ti_5O_{34}$

In contrast to the continuous change observed in the compositional range from β-Al_2TiO_5 to $Al_6Ti_2O_{13}$ the increase of only 2 mol% alumina leads to a sudden change clearly visible for weak reflections at low 2θ values (see Fig. 4). This observation suggests the formation of a new ordered compound, which is structurally related to $Al_6Ti_2O_{13}$ and should be richer in alumina. To limit the number of possible structural models which can be assembled by the described A and B blocks it was assumed that the reflections close to the positions of the 002 and 003 reflections of $Al_6Ti_2O_{13}$ (2θ equal to 13.6° and 21.9°, respectively) can be indexed with $00l_1$ and $00l_2$ ($l_1 \leqslant l_2, l_1 \geqslant 1, l_2 \geqslant 2$). It was found that a unit cell with a c-axis of $n * 32.5$ Å ($n = 1, 2, \ldots$) has theoretically reflections at these positions. Knowing the length of the new c-axis and assuming that the new compound should be richer in alumina than $Al_6Ti_2O_{13}$ the new compound should consist of n*(5A + 3B) blocks. Two models fulfill all mentioned requirements (Fig. 9). The first model consists of two unit cells of $Al_6Ti_2O_{13}$ followed by an A and B block. The second one can be figured by aligning five unit cells of $Al_6Ti_2O_{13}$ followed by a B block. Explicitly, it can be written like *A1B1A2-A1B1A2-**A1B1**-A2B2A1-A2B2A1-**A2B2*** (model 1, SG: Cmcm) and *A1B1A2-A1B1A2-A1B1A2-A1B1A2-A1B1A2-**B2*** (model 2, SG: Cm2m) where the deviations from the stacking found in $Al_6Ti_2O_{13}$ (*A1B1A2* or *A2B2A1*) are highlighted with bold letters.

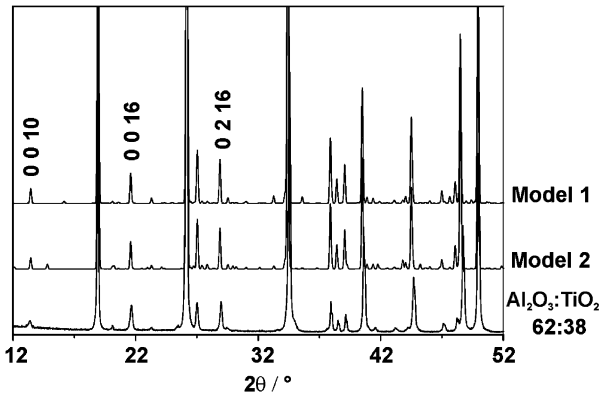

Fig. 8. Comparison of the X-ray powder patterns for the two proposed structural models for $Al_{16}Ti_5O_{34}$ with an experimental X-ray powder pattern obtained for a melted mixture consisting of Al_2O_3:TiO_2 62:38 mol%. The three reflections, which are highlighted in Fig. 4 are again marked and indexed with Miller's indices according to the structural models.

The stoichiometry of the new compound consisting of 5 A and 3 B blocks was calculated as follows: All together there are 42 cation sites and 68 oxygen atoms. Assuming that the trigonal-bipyramids are solely occupied by Al like in $Al_6Ti_2O_{13}$ [17] 36 cation sites remain which have to compensate 118 negative charges. That gives 26/36 Al and 10/36 Ti per mixed occupied cation site. The sum formula is then $Al_{16}Ti_5O_{34}$ or in terms of mol% 8 $Al_2O_3 \times 5$ $TiO_2 = 61.5\%$ Al_2O_3:38.5% TiO_2.

The calculated patterns and the measured one are shown in Fig. 8. Both models accounts well for the

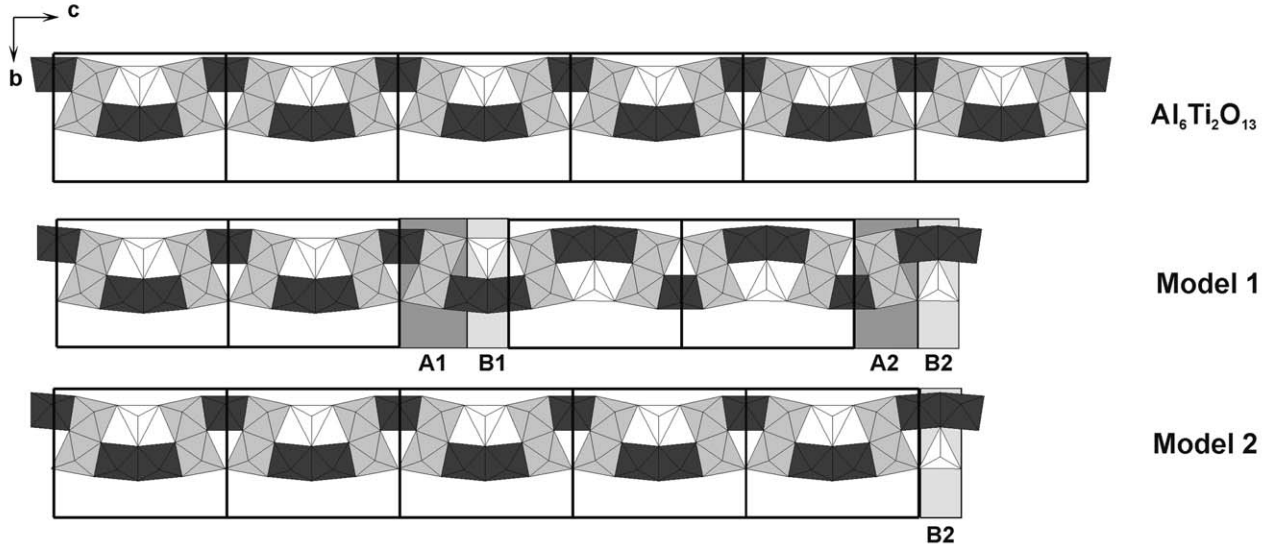

Fig. 9. The double chains of model 1 and model 2 proposed for the structure of $Al_{16}Ti_5O_{34}$ are shown and compared with $Al_6Ti_2O_{13}$ (six unit cells are outlined). The differences are highlighted in gray and the labels for the building blocks are given. The black rectangles correspond to the content of a unit cell $Al_6Ti_2O_{13}$.

observed change of the powder pattern when the alumina content is increase from 60 to 62 mol% (Fig. 4). The refined lattice parameters for model 1 (SG: Cmcm) are $a = 3.63995(9)$ Å, $b = 9.3107(3)$ Å, and $c = 65.321(2)$ Å and for model 2 (SG: Cm2m) $a = 3.6400(1)$ Å, $b = 9.3106(3)$ Å, and $c = 65.323(2)$ Å. A reliable distinction between these two models on the basis of the recorded powder patterns is not possible due to the limited resolution. The crystallographic data for both models are given in the Supplementary Material.

Another example for an IG consisting of pseudo-brookite blocks was recently reported by Grey et al. [28] who observed that the low-temperature oxidation of Anosovite (Ti_3O_5) leads to structures which can be described by Ti_3O_5 and anatase (TiO_2) blocks in a quite similar way.

4. Conclusions

This study shows that the recorded X-ray powder patterns obtained from annealed samples in the compositional range from Al_2O_3:TiO_2 48:52 to 62:38 mol% can be interpreted in terms of IG consisting of two basic building blocks which were derived from the recently determined structure of $Al_6Ti_2O_{13}$ [17]. This includes the ordered structures of β-Al_2TiO_5, $Al_6Ti_2O_{13}$ and the newly proposed structure of $Al_{16}Ti_5O_{34}$ as well as disordered structures derived from $Al_6Ti_2O_{13}$ (Fig. 10). From the available samples it cannot be ruled out that other ordered structures consisting of both blocks exist in the examined temperature range, which might be obtained after prolonged annealing in a narrow temperature range. However, the suggested model accounts well for the observed peak shifts and broadening especially for the 024 reflection ($Al_6Ti_2O_{13}$).

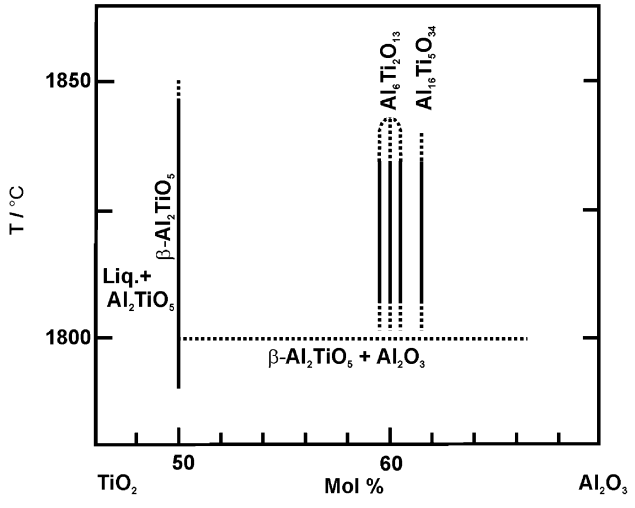

Fig. 10. Graphical representation of the experimental findings for the investigated compositional range in the system Al_2O_3–TiO_2.

The powder patterns provided no hints for the formation of α-Al_2TiO_5 [13] nor a structure with a c-axis of about 16.8 Å suggested by Mazerolles [16] but the new compound $Al_{16}Ti_5O_{34}$ could be identified which might be identically equal to a compound whose existence was proposed by Goldberg (labeled "Y" see Fig. 1) [2]. In agreement with this report it could be proved that $Al_6Ti_2O_{13}$ and $Al_{16}Ti_5O_{34}$ decompose during heating first into the binary oxides corundum and titania which react at higher temperatures to a mixture of β-Al_2TiO_5 and corundum.

Acknowledgments

SH acknowledge JSPS post doc fellowship No. P03752 and SN acknowledge JSPS post doc fellowship No. P03707. Dr. T. Watanabe and Dr. T. Ishigaki are kindly acknowledged for their help in recording powder XRD patterns.

Appendix A. Supplementary Materials

Supplementary data associated with this article can be found in the online version at doi:10.1016/j.jssc.2005.07.001

References

[1] B.G. Hyde, S. Andersson, Inorganic Crystal Structures, Wiley, New York, 1989.
[2] D. Goldberg, Rev. Int. Hautes Temper. Refract. 5 (1968) 181–194.
[3] A.E. Austin, C.M. Schwartz, Acta Crystallogr. 6 (1953) 812–813.
[4] L. Pauling, Z. Kristallogr. 73 (1930) 97–113.
[5] G. Bayer, J. Less-Common Met. 24 (1971) 129–138.
[6] H.W. Hennicke, W. Lingenberg, CFI: Ceramic Forum Int. 62 (1985) 439–445.
[7] T. Kameyama, T. Yamaguchi, Yogyo Kyokaishi 84 (1976) 589–593.
[8] E. Kato, K. Daimon, Y. Kobayashi, Yogyo Kyokaishi 86 (1978) 626–631.
[9] E. Kato, K. Daimon, J. Takahashi, J. Am. Ceram. Soc. 63 (1980) 355–356.
[10] E. Kato, Y. Kobayashi, K. Daimon, Yogyo Kyokaishi 87 (1979) 81–85.
[11] B. Morosin, R.W. Lynch, Acta Crystallogr. B 28 (1972) 1040–1046.
[12] T. Epicier, G. Thomas, H. Wohlfromm, J.S. Moya, J. Mater. Res. 6 (1991) 138–145.
[13] S.M. Lang, C.L. Fillmore, L.H. Maxwell, J. Res. NBS 48 (1952) 298–312.
[14] S.A. Azimov, D.D. Gulamova, N.N. Melnik, M.K. Sarkisova, S.K. Suleimanov, L.M. Tsapenko, Inorganic Mater.: A Translation of Izvestiya Akademii Nauk SSR 20 (1984) 399–401.
[15] H.A.J. Thomas, R. Stevens, Br. Ceram. Trans. J. 88 (1989) 144–151.

[16] L. Mazerolles, V. Bianchi, D. Michel, in: B. Jouffrey, C. Colliex (Eds.), Proceedings of the International Congress on Electron Microscopy, 1994, pp. 905–906.
[17] S.T. Norberg, S. Hoffmann, M. Yoshimura, N. Ishizawa, Acta Crystallogr. C61 (2005) i35–i38.
[18] T. Yamada, M. Yoshimura, S. Somiya, High Temp.-High Press. 18 (1986) 377–388.
[19] W. Gonschorek, Z. Kristallogr. 160 (1982) 187–203.
[20] N. Ishizawa, T. Miyata, I. Minato, F. Marumo, S. Iwai, Acta Crystallogr. B 36 (1980) 228–230.
[21] J. Rodriguez-Carvajal, in: (Eds.), Meeting on Powder Diffraction of the XV Congress of the IUCr, 1990, p. 127.
[22] K. Brandenburg, DIAMOND, 1999.
[23] M.M.J. Treacy, J.M. Newsam, M.W. Deem, Proc. R. Soc. Lond. A 433 (1991) 499–520.
[24] A.L. Spek, PLATON. A Multipurpose Crystallographic Tool, 2000.
[25] S.A. Azimov, D.D. Gulamova, M.K. Sarkisova, S.K. Suleimanov, Geliotekhnika 4 (1984) 11–13.
[26] A. Navrotsky, Am. Mineral. 60 (1975) 249–256.
[27] O. Yamaguchi, T. Hitoshi, K. Shimizu, Sci. Eng. Rev. Doshisha Univ. 22 (1981) 26–32.
[28] I.E. Grey, L.M.D. Cranswick, C. Li, T.J. White, L.A. Bursill, J. Solid State Chem. 150 (2000) 128–138.